Journal of Geosciences and Geomatics, 2020, Vol. 8, No. 2, 94-109
Available online at http://pubs.sciepub.com/jgg/8/2/5
Published by Science and Education Publishing
DOI:10.12691/jgg-8-2-5

Geochemistry of the Neoproterozoic Mbondo-Ngazi Tina Metasediments, Adamawa Area, Central Cameroon: Source Provenance and Tectonic Setting

Alexis Hamdja Ngoniri[1], Timoleon Ngnotue[1,*], Evine Laure Tanko Njiosseu[1], Patrick Ayonta Kenne[1], Sylvestre Ganno[2,*], Jean Paul Nzenti[2]

[1]Department of Earth Sciences, University of Dschang, P.O. Box. 67 Dschang, Cameroon
[2]Department of Earth Sciences, University of Yaoundé I, P.O. Box 812 Yaounde, Cameroon
*Corresponding authors: tngnotue@yahoo.fr, sganno2000@gmail.com

Received October 09, 2020; Revised November 10, 2020; Accepted November 17, 2020

Abstract The Mbondo-Ngazi Tina area belongs to the Adamawa-Yade domain within the Pan-African Central Africa Fold Belt in Cameroon (CAFB). The basement of this area is dominated by metasedimentary rocks composed of sericite schist, chlorite schist and muscovite schist. Whole-rock geochemical compositions of these rocks were investigated in order to determine their provenance and tectonic setting. The studied metasedimentary rocks have SiO_2 and Al_2O_3 contents comparable to the average composition of the Neoproterozoic upper continental crust (UCC). These rocks are strongly depleted in CaO, MgO, and enriched in K_2O, Ba and Rb with respect to UCC, reflecting K addition during diagenesis. The CIA, CIW, PIA and the SiO_2/Al_2O_3 and Th/U ratios indicated that these rocks had suffered varying degrees of weathering as the source rocks underwent mild to moderate chemical weathering. The PAAS-normalized REE patterns are almost flat with slightly LREE depletion with respect to HREE and null to weakly positive Eu anomalies. Their chondrite-normalized REE patterns are parallel to sub-parallel, LREE-enriched, and display distinct negative Eu anomalies and weakly fractionated HREE segments. Overall, they are geochemically mature and have suffered sedimentary recycling. They derived mainy from felsic to intermediate rocks with minor contamination of mafic rocks. The Mbondo-Ngazi Tina metasedimentary rocks show REE and trace element compositions similar to those of Archean sediments, suggesting that the continental crust of the study area during the early Proterozoic had chemical compositions similar to those of the Archean crust and were probably deposited in active to passive continental margin settings.

Keywords: *Metasediments, UCC, chemical weathering, Archean crust, Adamawa-Yade*

Cite This Article: Alexis Hamdja Ngoniri, Timoleon Ngnotue, Evine Laure Tanko Njiosseu, Patrick Ayonta Kenne, Sylvestre Ganno, and Jean Paul Nzenti, "Geochemistry of the Neoproterozoic Mbondo-Ngazi Tina Metasediments, Adamawa Area, Central Cameroon: Source Provenance and Tectonic Setting." *Journal of Geosciences and Geomatics*, vol. 8, no. 2 (2020): 94-109. doi: 10.12691/jgg-8-2-5.

1. Introduction

The Neoproterozoic crustal evolution of central Africa is characterized by the Pan-African orogeny [1,2,3,4]. This crustal evolution comprises the development of basins filled by volcano-sedimentary rocks, metamorphic rocks and by granitic intrusions. In Cameroon the Pan-African basement also known as Pan-African North Equatorial Fold Belt (PANEFB, [5,6]) or Central Africa Fold Belt (CAFB, [4]), is subdivided into three geodynamic domains that are disrupted and isolated from each other by transcurrent faults (Figure 1). Of these three domains, the central domain or Adamawa-Yade Domain (AYD) has been widely investigated for the past two decades, but their geodynamic evolution remains controversial and/or unrevealed. Many studies have been mainly concentrated on petrogenesis of granitoids which are widespread in the central domain [7-15] and only few works on the metamorphic rocks [7,16,17,18,19] In comparison to the granitoids, the metamorphic rocks, especially metasedimentary rocks from the central domain have received very little attention even though sedimentary rocks contain a wealth of information about provenance and crustal evolution [20,21]. It is now well established that detrital sediments contains part of a record of geologic history. Petrographic study has traditionally been an important method in extracting this information [22,23], but is not very useful for metamorphosed sediments. Geochemical investigations, particularly rare earth elements (REE) behaviors is a more suitable approach and can be effectively used for all types of clastic sediments, including metasediments, to evaluate the nature, the provenance and depositional setting [20].

In this paper, we examine the geochemistry of the Mbondo-Ngazi-Tina metasedimentary rocks located in the central domain of the Pan-African belt (Figure 1 and

Figure 2). The major purpose of this study is to constrain the source of the sediments and their tectonic setting.

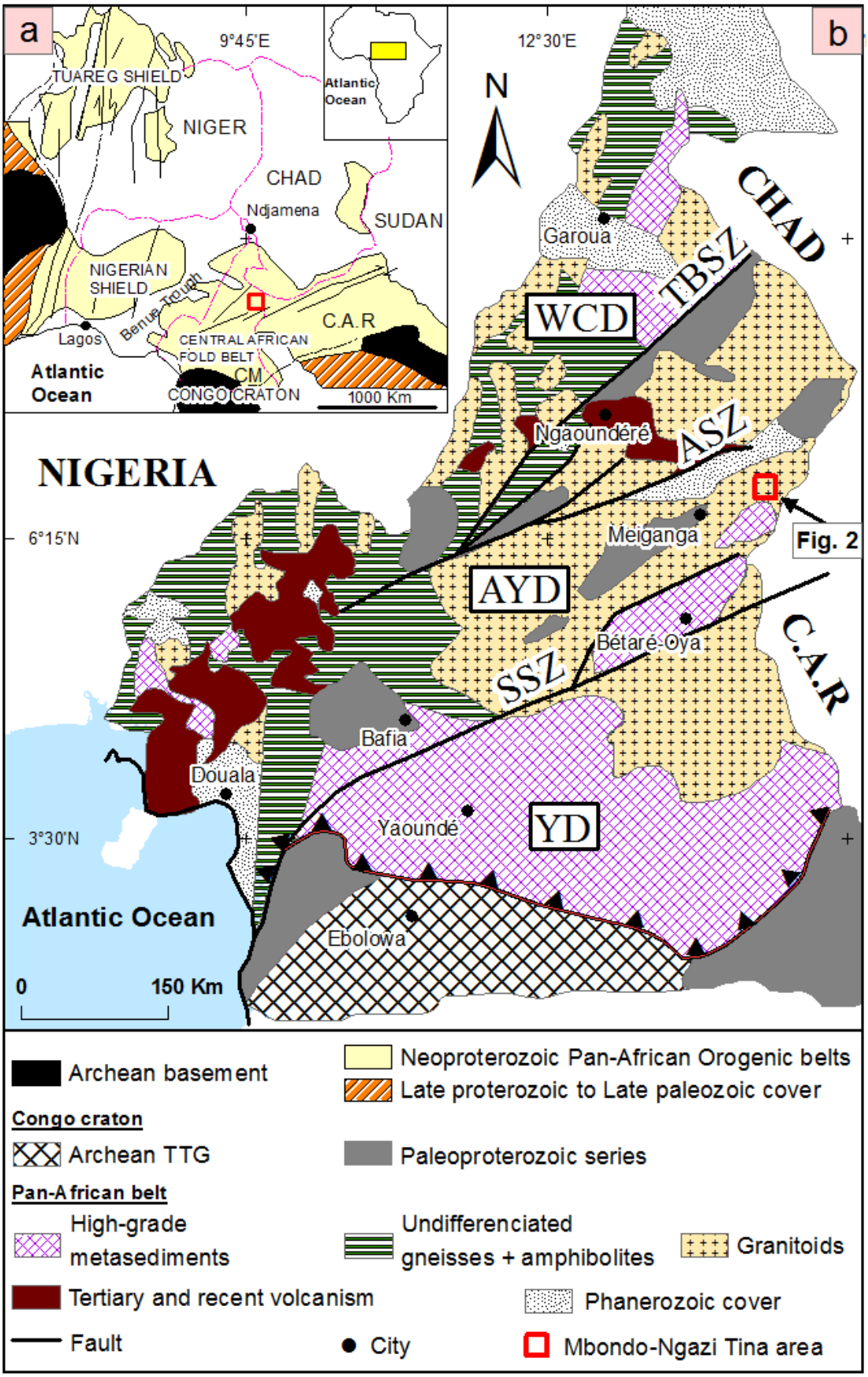

Figure 1. (a) Geological sketch map of west-central and north-east Brasil with cratonic masses and the Pan-African-Brasiliano provinces belt in west-Gondawana; (b) Geological map of Cameroon showing the major lithotectonic domains. WCD: West Cameroon Domain, AYD: Adamawa-Yadé domain, YD: Yaoundé Domain, TBSZ: Tcholliré-Banyo shear zone, ASZ: Adamaoua shear zone, SSZ: Sanaga shear zone. Location of study area is marked by a red square

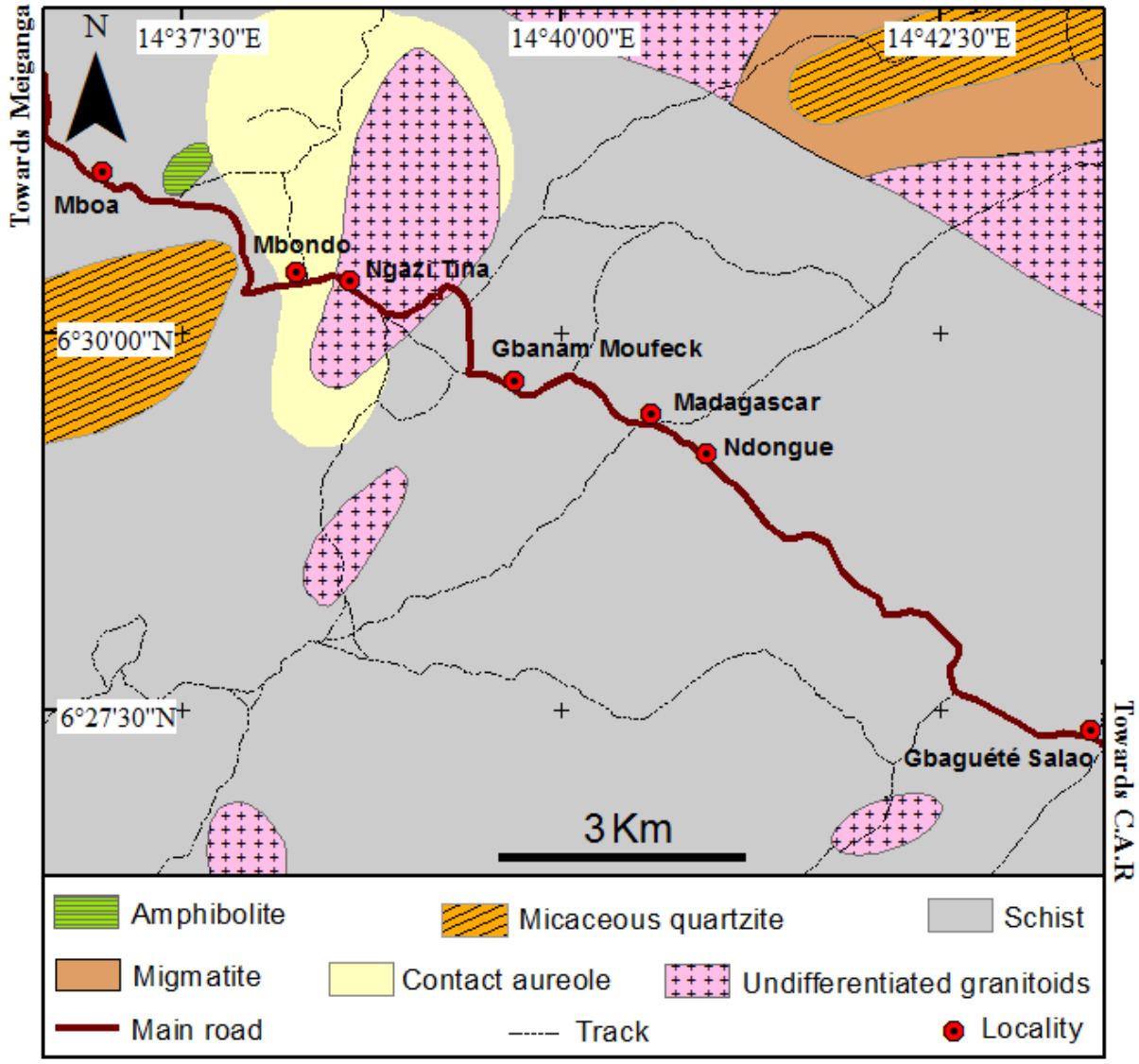

Figure 2. Geological sketch map of the Mbondo-Ngazi Tina area [32]

2. Geological Setting

The Central Africa Fold Belt is a major collisional belt that underlies the region from the West African Craton to East Africa [5,6,24]. It extends in parts of Nigeria to Uganda including Cameroon, Chad, Central African Republic and Sudan [24]. In Cameroon, this belt is divided into three litho-structural domains, namely the Yaoundé Domain (YD), Adamawa-Yadé Domain (AYD), and Northwestern Cameroon Domains (NWCD) (Figure 1) [4,25]. The YD consists of an extensive tectonic nappe that was thrusted onto the Congo Craton (CC) during the Pan-African collision [4,26,27]. Thrust slices of metasedimentary rocks with poorly constrained ages of ~626 Ma [28] are common in the Yaoundé Domain [6,25,29,30]. [27,31] suggested that the detrital material was derived from juvenile Palaeoproterozoic and Neoproterozoic sources in the southern part of the AYD, as well as from the Palaeoproterozoic Nyong Group in the CC. The Adamawa-Yade Domain is the largest domain dominated by syn- to late-collisional high-K calc-alkaline granitoids. These granitoids intrude high-grade gneisses that represent an Archean to Paleoproterozoic basement, which was likely dismembered during the Pan-African assembly of western Gondwanaland [16,17,19,25]. [4,28] classified the rocks of the AYD into three main groups: (a) Large supracrustal blocks of Paleoproterozoic metasedimentary rocks and orthogneisses with assimilated Archaean crust similar to the Ntem Complex, (b) 612-600 Ma, low- to medium grade metasedimentary and metavolcanoclastic rocks, and (c) 640- 610 Ma syn- to late-tectonic granitoids of transitional composition and crustal origin [25].

The Northwestern Cameroon Domain is located to the west of the Tcholliré-Banyo fault (TBF), along the western border of Cameroon and extends into eastern Nigeria. It includes a variety of rock types, namely (a) medium- to high-grade schists and gneisses of the ~700 Ma Poli series, (b) ~660-580 Ma calc-alkaline granitoids (diorite, granodiorite, and granite), (c) anorogenic alkaline granitoids, and (d) low-grade sedimentary and volcanic basin sequences [4,25].

It is generally believed that the CAFB was formed during the Neoproterozoic collision of the West African Craton with the Congo Craton. Toteu et al. [4] proposed a three-phase evolution, which began by the emplacement

of calc-alkaline granitic rocks (670-660 Ma), followed by crustal thickening, high-grade metamorphism, calc alkaline magmatism (640-610 Ma), and finally overprinted by post collision nappe formation, subalkaline to alkaline magmatism (600-545 Ma) and molasse basin sedimentation.

The Mbondo-Ngazi Tina area belongs to the eastern part of the AYD. This area comprises three groups of granitoids including granites, syenites and diorites, both showing I-type and metaluminous signatures. LA-ICP-MS U-Pb zircon analyses yield emplacement age of 576.4 ± 1.9 Ma and 585.9 ± 2.1 Ma for granites and syenites, respectively [32]. The dioritic rocks are ferroan and high-K calc-alkaline, while granites and syenites are magnesian and belong to the shoshonitic series. The Ti-in-zircon thermometer yields crystallization temperatures of 678-811°C and 658-768°C for granites and syenites, respectively [32]. These granitoids intrude meta-igneous and meta-sedimentary rocks composed of gneisses, amphibolites and schists (Figure 2). The meta-igneous and meta-sedimentary basement is locally covered by Cretaceous deposits (Mbéré-Djérem basin) and by Cenozoic volcanic rocks of the Cameroon Volcanic Line [33].

3. Analytical Methods

Twenty (eight sericite schists, three chlorite schists and nine muscovite schists) fresh rock samples were analyzed and data are presented in Table 1. Petrographic descriptions were carried out on polished thin sections prepared at Langfang Rock Detection Technology Services Ltd in Hebei, China. Whole rock geochemical analyses were performed at the Australian Laboratory Services (ALS) in Vancouver (Canada). The major elements were analyzed by inductively coupled plasma atomic emission (ICP-AES). This method consists of fixing a sample with a lithium metaborate-lithium tetraborate flux which also includes an oxidizing agent (Lithium Nitrate). The assembly will be cast in a platinum mould and then submitted for analysis. The uncertainty of the analysis of the major elements is 0.1-0.04%. Concerning trace and rare earth elements (REE), they have been analyzed by ICP-MS. This method consists of melting at 1025°C, a mixture of prepared sample and lithium metaborate/lithium tetraborate flux. Thus the result of the melted mixture was cooled and dissolved in a mixture of acids containing nitric, hydrochloric and hydrofluoric acids. The uncertainty of the analysis of trace elements and rare earth elements (REE) is 0.1-0.5%.

4. Petrography

4.1. Sericite Schists

Sericite schists crop out as balls and blocks of various sizes (60 × 80 cm; 0.9 × 1.5 m; Figure 3a). It is fine grained rock, greyish in color (Figure 3b) with heteroganular granoblastic microstructure. Mineral assemblage includes quartz, K-feldspar (orthoclase), sericite, epidote, plagioclase, and opaques (Figure 3c). Quartz (30-35%) occurs as smaller anhedral crystals associated with plagioclase. The later (20-25%) occurs as subhedral grains, associated with quartz and sericite flakes. These grains are sometimes grouped in clusters and often include opaque granules. Clusters of calcite are also observed in some sections. Quartz and calcite forms light layers that alternate with thin layers of sericite composition (Figure 3c). K-feldspar (25-30%) occurs as irregular subhedral to anhedral crystals associated with quartz. Some K-feldspar crystals host minute inclusions of sericite (Figure 3d). Sericite crystals are scarce and often present around the feldspar. Opaque minerals are subhedral and disseminated in the rock.

4.2. Chlorite Schists

Chlorite schist occurs along the river bed (Figure 3e). On the outcrop and hand specimen scale, the rock is fine grained, dark in color and display preferentially oriented quartz aggregates which are arranged in thin beds (Figure 3f). In thin sections, the rock exhibits lepidoblastic microstructure composed of quartz, chlorite, epidote and opaque minerals (Figure 3g). Quartz (40-45%) is the most abundant mineral phase of the rock. It is present either as subhedral crystals disseminated within the rock or as anhedral crystals forming clusters or pockets, molded by the chlorite flakes. Chlorite (25-30%) is in the form of lamellae or flakes that locally rimed the quartz aggregates. This mineral, together with secondary epidote (15-20%), form pronounced dark microbands (Figure 3g and Figure 3h).

4.3. Muscovite Schists

Muscovite schists crop out in the bed of the river Taparé, Wàn deh and Gboum (Figure 3i). The rock is dark in color with luster appearance (Figure 3j), and display granonematoblastic microstructure composed of quartz, plagioclase, muscovite, calcite, and opaques (Figure 3k and Figure 3l). Quartz (25-30%) occurs as irregular subhedral to anhedral crystals dispersed within the rock mass. Plagioclase (15-20%) appears as subhedral to anhedral crystals, generally associated with quartz. Muscovite (15-25%) occurs as subhedral to anhedral flakes that are preferentially oriented. Calcite (5-10%) appears as grains dispersed in the rock and often associated with quartz and plagioclase crystals. Opaque minerals are abundant (8-10%) and occur as euhedral to subhedral grains, disseminated in the rock or embedded in muscovite flakes.

5. Geochemistry

Whole-rock geochemical data of representative fresh rock samples of the Mbondo-Ngazi Tina metasedimentary rocks is given in Table 1. In the Zr/Ti vs Ni protolith discrimination diagram of [34], the investigated samples fall within the sedimentary field (Figure 4a). The classification diagram of [35] reveals that the Mbondo-Ngazi Tina metasedimentary rocks correspond to Fe-sand (chlorite schists), shale (muscovite schists) and arkose (sericite schists) (Figure 4b).

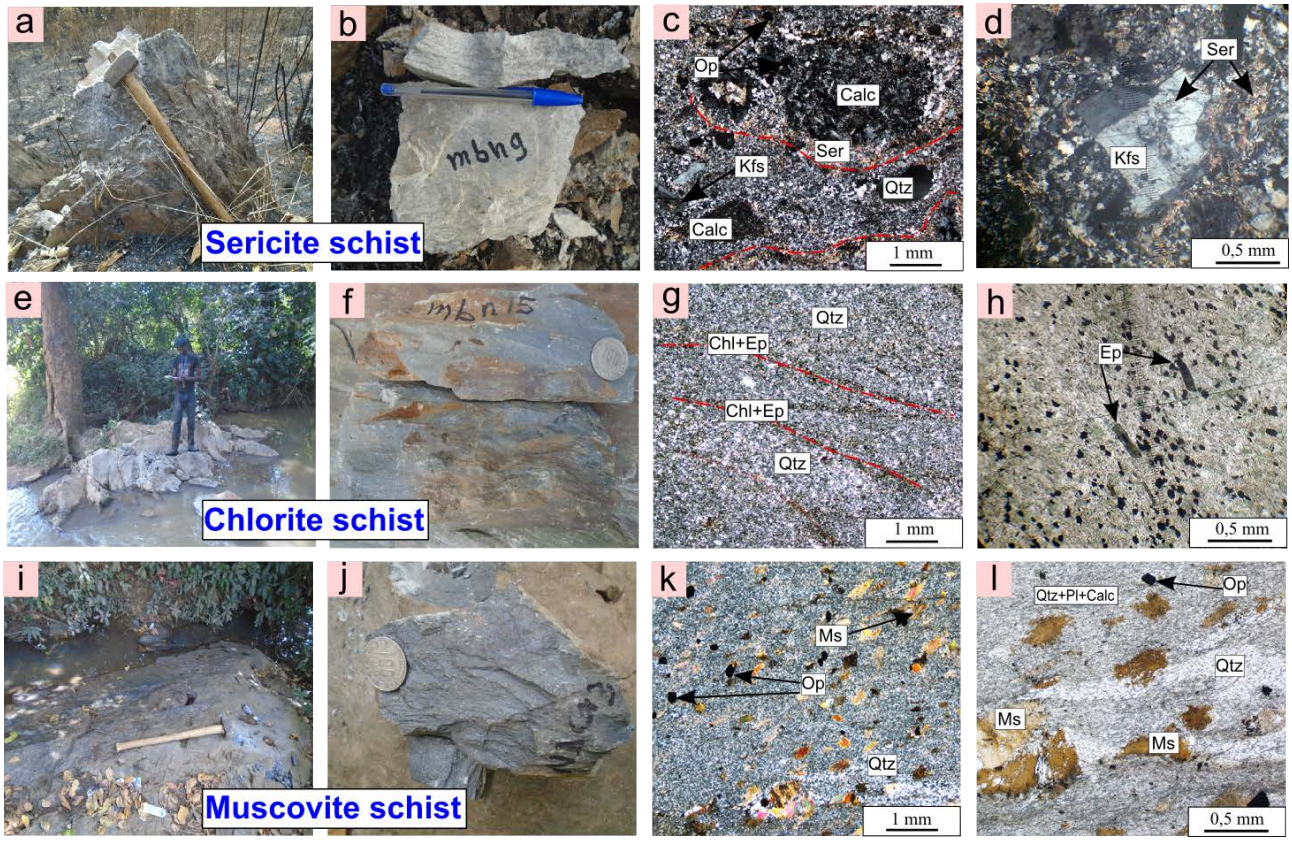

Figure 3. Photographs [outcrop (a, e, i) and hand specimen views (b, f, j)] and microphotographs (c, d, g, h, k, l) of the Mbondo-Ngazi Tina metsaediments. Abbreviations: Calc: Calcite; Chl: Chlorite; Ep: Epidote; Kfs: K-feldspar; Qtz: Quartz; Ms: Muscovite; Ser: sericite; Op: Opaque minerals

Table 1. Major element concentrations (in wt%) of the Mbondo-Ngazi Tina metasedimentary rocks

Rocks	Sericite schists								Chlorite schists			Muscovite schists								
Samples	MBN8	MBN4a	MBN4b	MBN4c	MBN11a	MBN11b	MBN9a	MBN9b	MBN15a	MBN15b	MBN15c	NDG2a	NDG2b	NDG2c	NDG3a	NDG3b	NDG3c	SAL8a	SAL8b	SAL8c
SiO_2	80.8	86	83.4	83.7	76.4	73.8	70.9	65.1	68.4	72.9	72.8	61	61.4	59.2	58.2	59.3	56.4	63.9	62.9	62.8
Al_2O_3	9.62	7.23	8.52	8.21	14.65	14.3	16.35	19.7	13.05	10.4	10.85	17.2	17	18.05	18.45	17.35	18.5	17.15	17	17.2
Fe_2O_3	1.79	1.66	1.94	2.16	1.95	2.71	2.05	2.73	7.57	7.94	7.4	8.49	8.33	8.16	8.41	8.22	8.45	7.5	7.52	7.29
CaO	0.01	0.05	0.03	0.04	0.02	0.13	0.01	0	0.35	0.27	0.28	1.3	1.22	1.07	1.04	1.2	1.04	0.12	0.1	0.13
MgO	0.13	0.31	0.36	0.36	0.55	0.74	1.22	1.45	2.14	1.92	1.89	3.97	3.92	3.87	4.15	3.9	4.1	2.2	2.2	2.17
Na_2O	0.06	0.02	0.03	0.02	0.11	0.12	0.04	0.05	2.48	2.03	2.14	2.67	2.53	2.31	2.39	2.56	2.44	1.31	1.32	1.37
K_2O	6.42	2.97	3.6	3.36	4.8	4.69	6.07	7.31	2.02	1.37	1.51	2.62	2.71	3.09	3.16	2.52	3.17	2.85	2.78	2.86
Cr_2O_3	0.004	0.054	0.004	0.006	0.021	0.004	0.021	0.003	0.018	0.014	0.014	0.019	0.02	0.018	0.019	0.019	0.028	0.017	0.017	0.018
TiO_2	0.15	0.21	0.24	0.2	0.27	0.4	0.28	0.33	1.05	0.89	0.9	1.04	1.02	0.98	0.96	0.95	1	0.92	0.89	0.92
MnO	0.01	0.02	0.02	0.02	0.01	0.02	0.03	0.04	0.12	0.11	0.13	0.12	0.11	0.12	0.12	0.12	0.12	0.06	0.06	0.06
P_2O_5	0.12	0.09	0.08	0.07	0.08	0.14	0.04	0.07	0.24	0.2	0.19	0.27	0.27	0.24	0.25	0.25	0.24	0.12	0.11	0.11
SrO	<0.01	<0.01	<0.01	<0.01	0.01	<0.01	<0.01	<0.01	<0.01	0.01	<0.01	0.02	0.02	0.02	<0.01	0.01	0.01	<0.01	<0.01	<0.01
BaO	0.29	0.12	0.15	0.13	0.14	0.13	0.23	0.27	0.09	0.06	0.07	0.05	0.06	0.07	0.07	0.07	0.07	0.09	0.09	0.09
LOI	1.05	1.58	1.52	1.55	2.46	2.32	2.84	3.35	2.71	2.51	2.34	2.99	2.99	3.37	3.59	3.69	4.24	4.75	4.68	4.52
Total	100.45	100.31	99.89	99.83	101.47	99.5	100.08	100.4	100.24	100.62	100.51	101.76	101.6	100.57	100.81	100.16	99.81	100.99	99.67	99.54
K_2O+Na_2O	6.48	2.99	3.63	3.38	4.91	4.81	6.11	7.36	4.50	3.40	3.65	5.29	5.24	5.40	5.55	5.08	5.61	4.16	4.10	4.23
K_2O/Na_2O	107.00	148.50	120.00	168.00	43.64	39.08	151.75	146.20	0.81	0.67	0.71	0.98	1.07	1.34	1.32	0.98	1.30	2.18	2.11	2.09
CIA	59.71	70.40	69.95	70.59	74.82	74.32	72.76	72.80	72.91	73.92	73.41	72.30	72.46	73.61	73.68	73.42	73.56	80.03	80.19	79.78
CIW	59.94	70.54	70.12	70.71	75.24	74.79	72.89	72.94	84.63	86.38	85.84	81.44	81.22	81.27	81.46	82.34	81.46	85.24	85.51	85.19
PIA	97.86	98.38	98.80	98.78	98.70	97.46	99.52	99.60	79.58	79.70	79.42	78.60	79.21	81.57	81.68	79.77	81.50	90.91	90.92	90.53

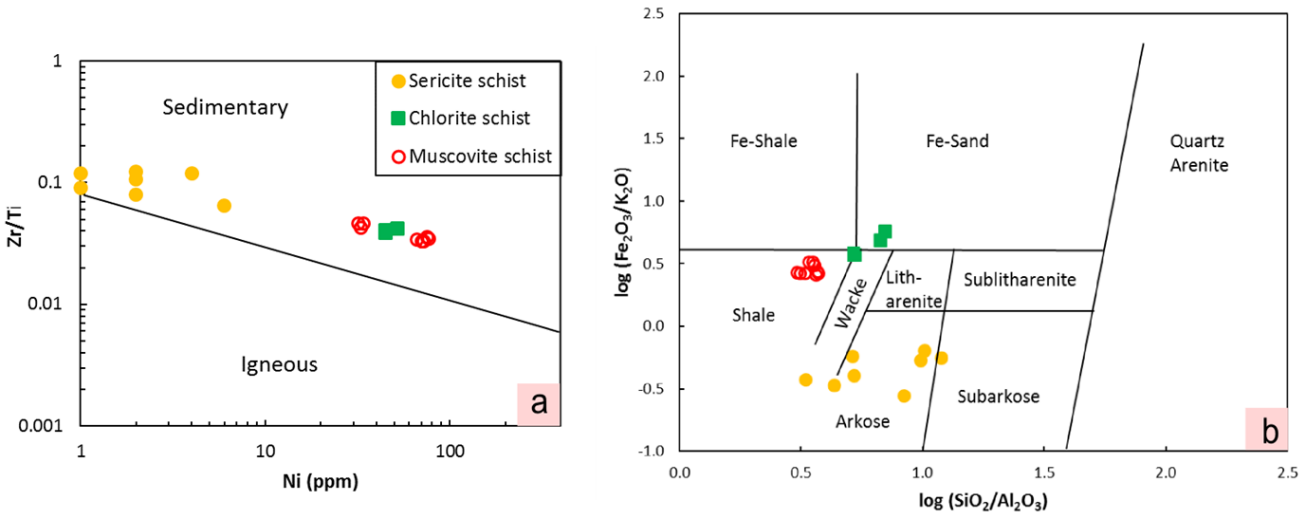

Figure 4. a) Zr/Ti vs Ni protolith discrimination diagram [34]; b) Sediment classification diagram [35]

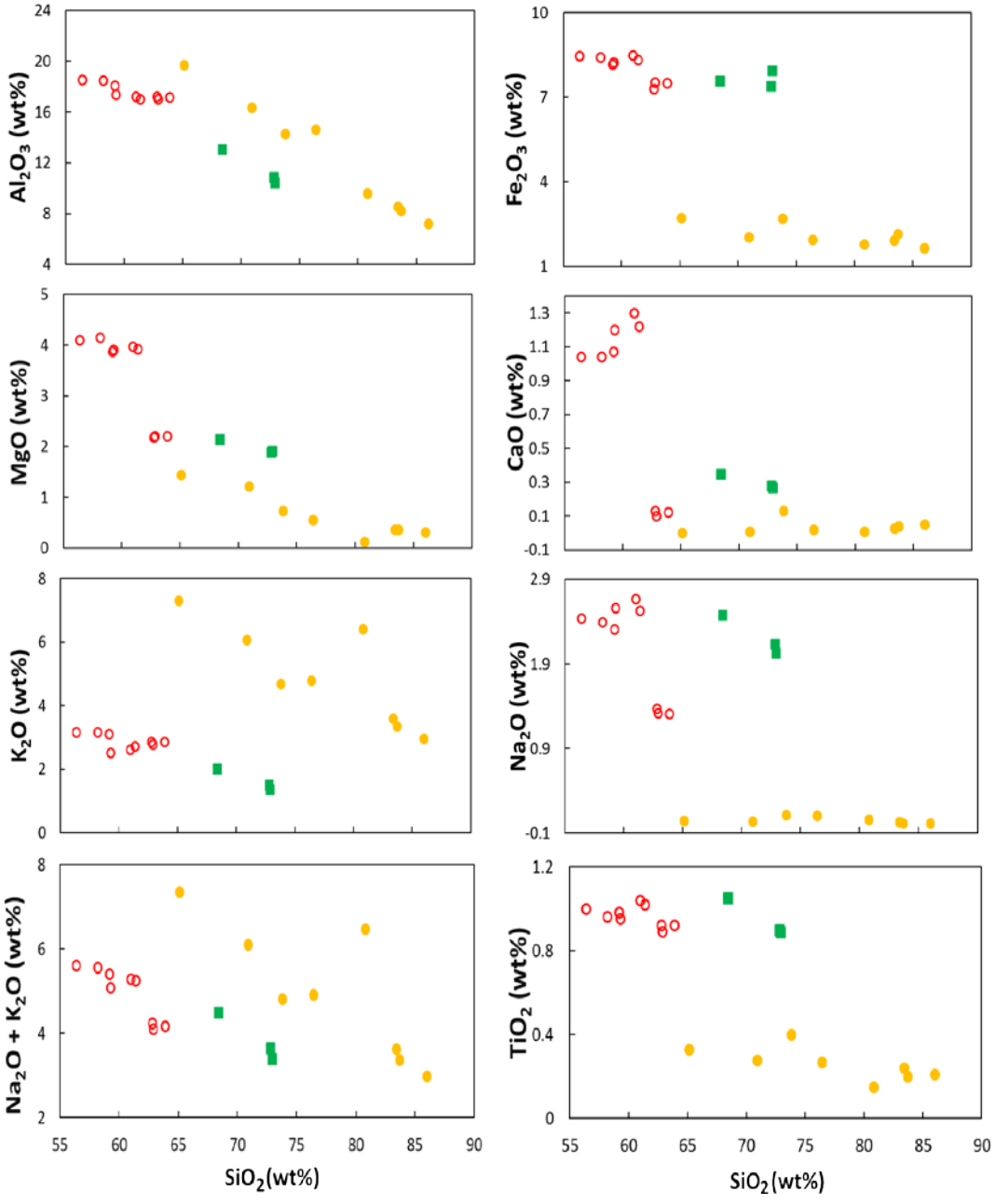

Figure 5. Harker diagrams of selected major elements

5.1. Major Elements

Sericite schists are characterized by very high SiO_2 contents with values ranging between 65.1 and 86 wt%. The Al_2O_3 contents are moderate to high (7.23-19.7 wt%) while Fe_2O_3 (1.66-2.73 wt%), MgO (0.13-1.45 wt%) and TiO_2 (0.15-0.4 wt%) contents are low. Total alkali ($2.99 < Na_2O+K_2O < 7.36$ wt%) contents are low to moderate. The K_2O/Na_2O ratio is very high (39.08-168) suggesting a very high detrital feldspar rich component. Other oxide contents such as CaO (0-0.13 wt%), Cr_2O_3 (0.003-0.054 wt%), MnO (0.01-0.04 wt%) and P_2O_5 (0.04-0.14 wt%) contents are negligible in the rock.

Chlorite schist samples are characterized by high contents of SiO_2 (68.4-72.9 wt%), but their Al_2O_3 (10.4-13.05 wt%) and Fe_2O_3 (7.4-7.94 wt%) concentrations are moderate. The MgO and TiO_2 concentrations are low and range from 1.89 to 2.14 wt%, 0.89 to 1.05 wt% respectively. This rock also exhibits low alkali elements ($3.4 < Na_2O+K_2O < 4.5$ wt%) and low K_2O/Na_2O ratio (0.67-0.81). CaO, Cr_2O_3, MnO and P_2O_5 contents are very low; with values ranging from 0.27 to 0.35 wt%, from 0.014 to 0.018 wt%, from 0.11 to 0.13 and from 0.19 to 0.24 wt%, respectively.

Muscovite schists have moderate to high contents of SiO_2 (56.4-63.9 wt%). These rocks are enriched in Al_2O_3 (16-18.5 wt%) and Fe_2O_3 (7.29-8.49 wt%) and depleted in TiO_2 (0.89-1.04 wt%) and CaO (0.1-1.3 wt%). Their MgO (2.17-4.15 wt%) and total alkali ($4.1 < Na_2O+K_2O < 5.61$) contents is slightly high when compared to those of chlorite schists. The K_2O/Na_2O values are low and range from 0.98 to 2.17. The others oxides (Cr_2O_3, MnO, P_2O_5) display very low content (less than 0.5 wt%).

Variations in the major element oxides of the studied metasediments are showed on Harker diagrams (Figure 5). Overall, the diagrams display negative correlations with Al_2O_3, Fe_2O_3, MgO, K_2O and TiO_2. When compared to the international standards (i.e. Post-Archean Australian Shale, PAAS; North American Shale Composite, NASC and Upper Continental Crust, UCC), the studied schists are characterized by high SiO_2 and low MgO, Fe_2O_3 and CaO contents. Their average Al_2O_3 content (13.32 wt%; 11.43 wt%, 17.54 wt% for sericite schists, chlorite schist and muscovite schists respectively) are similar to that of international reference suggesting low clay content. However, the average abundances of the other major element oxides are more or less comparable to the reference compositions presented in Table 3.

Table 2. Trace and rare earth element compositions (in ppm) of the Mbondo-Ngazi Tina metasedimentary rocks

Rocks	Sericite schists								Chlorite schists			Muscovite schists								
Samples	MBN8	MBN4a	MBN4b	MBN4c	MBN11a	MBN11b	MBN9a	MBN9b	MBN15a	MBN15b	MBN15c	NDG2a	NDG2b	NDG2c	NDG3a	NDG3b	NDG3c	SAL8a	SAL8b	SAL8c
Cs	2.88	2.13	2.3	2.39	7.38	6.95	7.03	9.01	2.21	1.44	1.62	6.2	6.19	5.79	5.95	3.89	6.79	5.23	5.09	5.4
Rb	159.5	101.5	110	114	127	122.5	170.5	213	79.6	55.3	58	87.1	90.7	98.8	96.2	77.6	97.7	117.5	119	121.5
Ba	2800	1075	1295	1185	1305	1225	2050	2530	777	535	613	466	502	637	651	582	627	771	799	799
Th	3.86	2.96	3.49	3.31	6.31	5.01	7.33	8.1	9.29	7.07	7.25	7.04	7.13	7.31	7.35	7.24	6.94	10.7	10.5	10.75
Zn	18	55	50	60	42	78	91	106	123	114	108	129	125	109	118	117	122	63	63	69
U	1.43	1.08	1.64	1.22	1.58	1.74	0.93	0.98	2.04	1.69	1.6	2.76	2.54	2.69	3.23	2.55	2.94	2.6	2.61	2.55
Nb	5.4	4.8	4.3	4.7	8.4	5.2	8.4	11.6	17.4	15.4	14.7	11.3	11	8.3	9.7	9.1	9.7	14.7	14.7	15.2
Ta	<0.1	<0.1	0.4	<0.1	0.2	0.5	0.7	0.3	0.8	0.6	0.6	0.3	0.3	0.6	0.2	0.2	0.2	0.9	1	1
Cr	10	380	10	20	160	10	130	<10	120	90	80	130	120	120	140	120	180	110	110	110
Ni	2	2	2	1	4	6	1	<1	52	45	45	72	71	66	75	71	77	33	34	32
Co	<1	1	1	<1	3	6	1	1	21	21	20	18	16	11	22	16	21	9	12	11
La	11.2	8.9	13.2	11.1	31.6	23.9	26.9	37	30.7	27.4	27.5	36.1	31.3	23.5	34.2	19	29.8	39.7	39.2	39.5
Ce	26.3	16.1	24.1	21.5	64.1	47.9	53.7	65.7	63	52.6	49.9	62.6	58.2	50.3	64.7	39.8	57.9	81.2	82.4	80.8
Pr	3.18	2.12	3.34	2.8	8.21	6.38	6.06	8.32	7.55	6.24	6.43	8.95	7.67	6.49	8.59	5.17	7.61	9.12	9.24	9.1
Sr	39.5	12.9	17.6	13.9	66.7	62.9	23.9	28.1	135.5	103.5	108.5	269	251	231	247	265	248	48.8	48.8	50.9
Nd	13.5	9.4	13.9	11.8	33.6	26.6	24.1	32.6	30.5	26.1	25.3	36.9	31.2	27.3	36.3	21.5	30.9	35.6	35.8	35.2
Zr	110	135	114	108	193	156	199	236	266	215	209	204	202	199	206	187	207	235	246	253
Hf	2.6	3.1	3.2	2.8	4.6	4.1	5.2	5.8	6.7	5.3	5.3	5.2	5.3	5.1	5.4	4.8	5.2	6.7	6.8	6.8
Sm	3.36	2.01	3.14	2.55	6.58	5.52	4.63	5.86	6.15	5.53	5.14	7.65	6.72	6.53	7.63	5.18	6.73	7.41	7.08	7.06
Eu	0.91	0.54	0.74	0.61	1.27	1.05	1.13	1.34	1.21	1.15	1.02	1.58	1.56	1.32	1.64	1.29	1.59	1.56	1.51	1.42
Gd	3.28	2.1	2.54	2.48	5.85	5.05	3.63	4.46	5.4	4.48	4.72	6.67	6.56	5.4	6.36	4.87	5.95	5.84	5.54	5.92
Tb	0.49	0.33	0.47	0.43	0.97	0.89	0.64	0.84	0.93	0.81	0.78	1.09	1.07	0.95	1.04	0.84	0.96	0.91	0.89	0.93
Dy	2.92	1.92	2.74	2.71	5.96	5.03	3.96	4.97	5.35	4.63	4.44	6	6.01	5.54	6	5.3	5.59	5.64	5.45	5.86
Ho	0.58	0.46	0.55	0.58	1.37	1.21	0.84	1.11	1.08	0.92	0.94	1.35	1.31	1.23	1.32	1.18	1.23	1.18	1.15	1.19
Er	1.77	1.51	1.95	1.87	4.36	3.62	2.68	3.4	3.35	2.74	2.76	4.07	3.72	3.59	3.65	3.77	3.66	3.28	3.63	3.7
Yb	1.92	1.43	2.04	1.96	4.05	3.61	3.08	3.86	3.11	2.59	2.64	3.51	3.35	3.31	3.68	3.22	3.46	3.3	3.56	3.44
Y	19	14.9	19.1	19.5	43.5	34.9	23.8	34.8	30.1	26.5	25.5	36.2	35.3	32.8	36	31.3	34.4	31.8	32.9	33.6
Lu	0.32	0.24	0.3	0.34	0.7	0.61	0.49	0.61	0.51	0.43	0.43	0.57	0.56	0.53	0.59	0.53	0.51	0.56	0.53	0.52
Th/U	2.7	2.74	2.13	2.71	3.99	2.88	7.88	8.27	4.55	4.18	4.53	2.55	2.81	2.72	2.28	2.84	2.36	4.12	4.02	4.22
La/Th	2.9	3.01	3.78	3.35	5.01	4.77	3.67	4.57	3.3	3.88	3.79	5.13	4.39	3.21	4.65	2.62	4.29	3.71	3.73	3.67
Th/Sc	1.93	0.99	0.87	0.83	1.05	0.63	1.47	1.35	0.66	0.64	0.66	0.35	0.36	0.33	0.33	0.34	0.32	0.59	0.58	0.6
Zr/Sc	55	45	28.5	27	32.17	19.5	39.8	39.33	19	19.55	19	10.2	10.1	9.05	9.36	8.9	9.41	13.06	13.67	14.06
La_N/Yb_N	0.43	0.46	0.48	0.42	0.58	0.49	0.64	0.71	0.73	0.78	0.77	0.76	0.69	0.52	0.69	0.44	0.64	0.89	0.81	0.85
La_N/Sm_N	0.48	0.64	0.61	0.63	0.7	0.63	0.84	0.92	0.73	0.72	0.78	0.69	0.68	0.52	0.65	0.53	0.64	0.78	0.8	0.81
Gd_N/Yb_N	1.03	0.89	0.75	0.77	0.87	0.85	0.71	0.7	1.05	1.05	1.08	1.15	1.19	0.99	1.05	0.92	1.04	1.07	0.94	1.04
Eu/Eu*	1.31	1.15	1.06	0.98	0.9	0.85	1.09	1.02	1.01	1.11	1.01	1.12	1.2	1.04	1.13	1.15	1.21	1.15	1.1	1.06

Normalized values are from [62].

Table 3. Average major and trace element compositions of the Mbondo-Ngazi Tina metasediments and other Precambrian sediments from international references

Rocks	Sericite schist (n=8)	Chlorite schist (n=3)	Muscovite schist (n=9)	PAAS[a]	NASC[b]	UCC[c]
SiO_2	77.07	71.37	60.57	62.8	64.8	66.6
TiO_2	0.3	0.95	0.96	1	0.7	0.64
Al_2O_3	12.1	11.43	17.54	18.9	16.9	15.4
Fe_2O_3	2.42	7.64	8.04	6.5	5.67	5.04
MnO	0.02	0.12	0.1	0.11	0.06	0.1
MgO	0.61	1.98	3.39	2.2	2.86	2.48
CaO	0.07	0.3	0.8	1.3	3.63	3.59
Na_2O	0.06	2.22	2.1	1.2	1.14	3.27
K_2O	5.1	1.63	2.86	3.7	3.97	2.8
P_2O_5	0.11	0.21	0.21	0.16	0.13	0.15
Total	100.05	97.85	96.57	97.81	97.87	99.86
Sc	5.67	12	20.11	16	15	14
V	23	86.67	178.67	150	130	97
Cr	91.25	96.67	126.67	110	125	92
Co	2.14	20.67	15.11		26.35	17.3
Ni	2.5	47.33	59	55	58	47
Cu	3.14	20.33	36.56			28
Zn	66.22	115	101.67			67
Ga	15.16	15.03	23.81			17.5
Rb	145.06	64.3	100.68	160	125	84
Sr	33.37	115.83	184.39	200	142	320
Cs	5.07	1.76	5.61	15	5.16	4.9
Ba	1647.22	641.67	648.22	650	636	624
Nb	6.34	15.83	11.52	19	13	12
Ta	0.42	0.67	0.52	1.28	1.12	0.9
Zr	150.56	230	215.44	210	200	193
Hf	3.72	5.77	5.7	5	6.3	5.3
U	1.29	1.78	2.72	3.1	2.7	2.7
Th	4.7	7.87	8.33	14.6	12.3	10.5
Pb	19.44	8	14.33	20	20	17
La	19.74	28.53	32.48	38.2	31.1	31
Ce	38.62	55.17	64.21	79.6	67	63
Pr	4.94	6.74	7.99	8.83		7.1
Nd	20.46	27.3	32.3	33.9	30.4	27
Sm	4.19	5.61	6.89	5.55	5.98	4.7
Eu	0.99	1.13	1.5	1.08	1.25	1
Gd	3.69	4.87	5.9	4.66	5.5	4
Tb	0.63	0.84	0.96	0.77	0.85	0.7
Dy	3.73	4.81	5.71	4.68	5.54	3.9
Ho	0.82	0.98	1.24	0.99		0.83
Er	2.59	2.95	3.67	2.85	3.28	2.3
Yb	2.66	2.78	3.43	2.82	3.11	2
Y	25.67	27.37	33.81	27	35	21
Lu	0.43	0.46	0.54	0.43	0.46	0.31
Sum REE	129.16	169.52	200.64	211.36	189.47	168.84
Eu/Eu^*_{PAAS}	1.11	1.04	1.12	1	1.06	1.19
Eu/Eu^*_{CN}	0.79	0.73	1.02	0.7	0.75	0.81

[a]PAAS = Post-Archean Australian Shale [62]; [b]NASC = North American shale composite [63]; [c]UCC = upper continental crust [64].

5.2. Trace and Rare Earth Elements (REE)

Trace elements and rare earth elements compositions of the Mbondo-Ngazi-Tina metasedimentatry rocks are listed in Table 2. The sericite schists are characterized by high Ba (1075-2800 ppm), Rb (101.5-213 ppm) and Zr (108-236 ppm) contents. Nd (9.4-33.6 ppm), Zn (18-106 ppm), Sr (12.9-66.7 ppm), Y (14.9-43.5 ppm), Cr (<10-380 ppm) and Cs (2.13-9.01 ppm) contents are moderate to low while Ni (<1-6 ppm) and Co (<1-6 ppm) concentrations are very low. The variation diagrams of some trace elements with silica show negative correlation (Figure 6). The UCC-normalized trace element patterns shows negative anomalies in Ni, Sc, Sr, Ce and while Ba, Zr and Y displayed positive anomalies (Figure 7a). The PAAS-normalized REE pattern shows LREE depletion [$(La/Yb)_N$ =0.42-0.71] relative to HREE [$(Gd/Yb)_N$ =0.70-1.03] with null to slightly positive Eu anomalies (Eu/Eu*=0.85-1.31) (Figure 7b).

Chlorite schist samples are enriched in Ba and Zr, with values ranginess from 535 to 777 ppm and from 266 to 209 ppm, respectively. They are moderately rich in Sr (103.5-135.5 ppm), Zn (108-123 ppm) and Cr (80-120 ppm). These chlorite schists are slightly poor in Rb (53.3-79.6 ppm), Ni (45-52 ppm), Y (25.5-30.1 ppm), Nd (25.3-30.5 ppm), Co (20-21 ppm) and very poor in Cs (1.44-2.21 ppm). Binary variation plots of some trace elements with SiO_2 exhibit negative correlations with Ba, Sr, Zr, Rb, Y, Nd and Cs (Figure 6). The multi-elements spider diagrams show negative anomalies in Rb, Sr, Ce and Ho and positive anomalies in Co, Ba, Zr and Tm (Figure 7c). Their PAAS-normalized REE patterns are relatively flat and lack of Eu anomaly (Eu/Eu* =1.01-1.11). They show weak HREE enrichment [$(Gd/Yb)_N$=1.05-1.08] with respect to LREE [$(La/Sm)_N$=0.72-0.78] (Figure 7d).

Muscovite schists are enriched in Ba and Zr, with values ranging from 466-799 ppm and 187-253 ppm, respectively. Their Cr (110-180 ppm), Sr (48.8-269 ppm), Rb (87.1-121.5 ppm) and Zn (63-129 ppm) contents are moderate to high, while Ni (32-77 ppm), Y (31.3-36.2 ppm), Nd (21.5-36.9 ppm), Co (9-22 ppm) and Cs (3.89-6.79 ppm) contents are low. The variation diagrams of some trace elements against SiO_2 shows positive correlations with Ba, Zr, Rb and Nd, whilst negative correlations are observed with Zn, Y and Cs (Figure 6). The UCC-normalized multi-elements patterns of the studied rock are quite similar, with the exception of a pronounced Co negative anomaly observed in muscovite schist samples (Figure 7e). Their PAAS-normalized REE patterns are flat, with slightly LREE depletion [$(La/Yb)_N$=0.44-0.89] relative to HREE [$(Gd/Yb)_N$=0.92-1.19] (Figure 7f).

When normalized to chondrite, the Mbondo-Ngazi Tina metasediments display enrichment in LREE relative to HREE, and negative Eu anomalies (Eu/Eu*=0.56-0.93). The REE patterns of the studied rocks are comparable to those of UCC and PAAS (Figure 8). They are moderately fractionated with LREE enrichment [$(La/Sm)_N$=2.08-4.92] relative to HREE [$(Gd/Yb)_N$= 0.89-1.58].

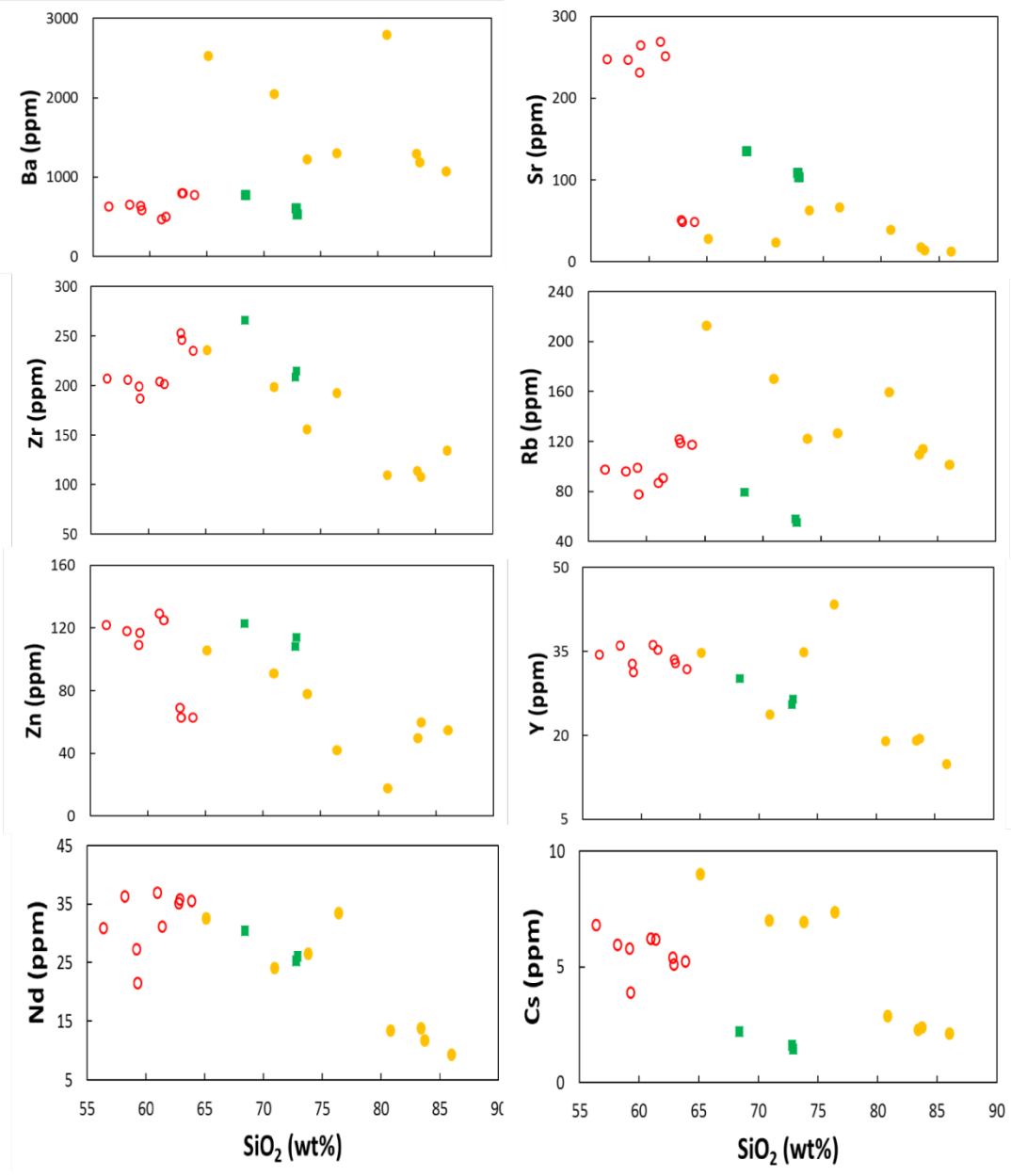

Figure 6. Harker diagrams of selected trace elements

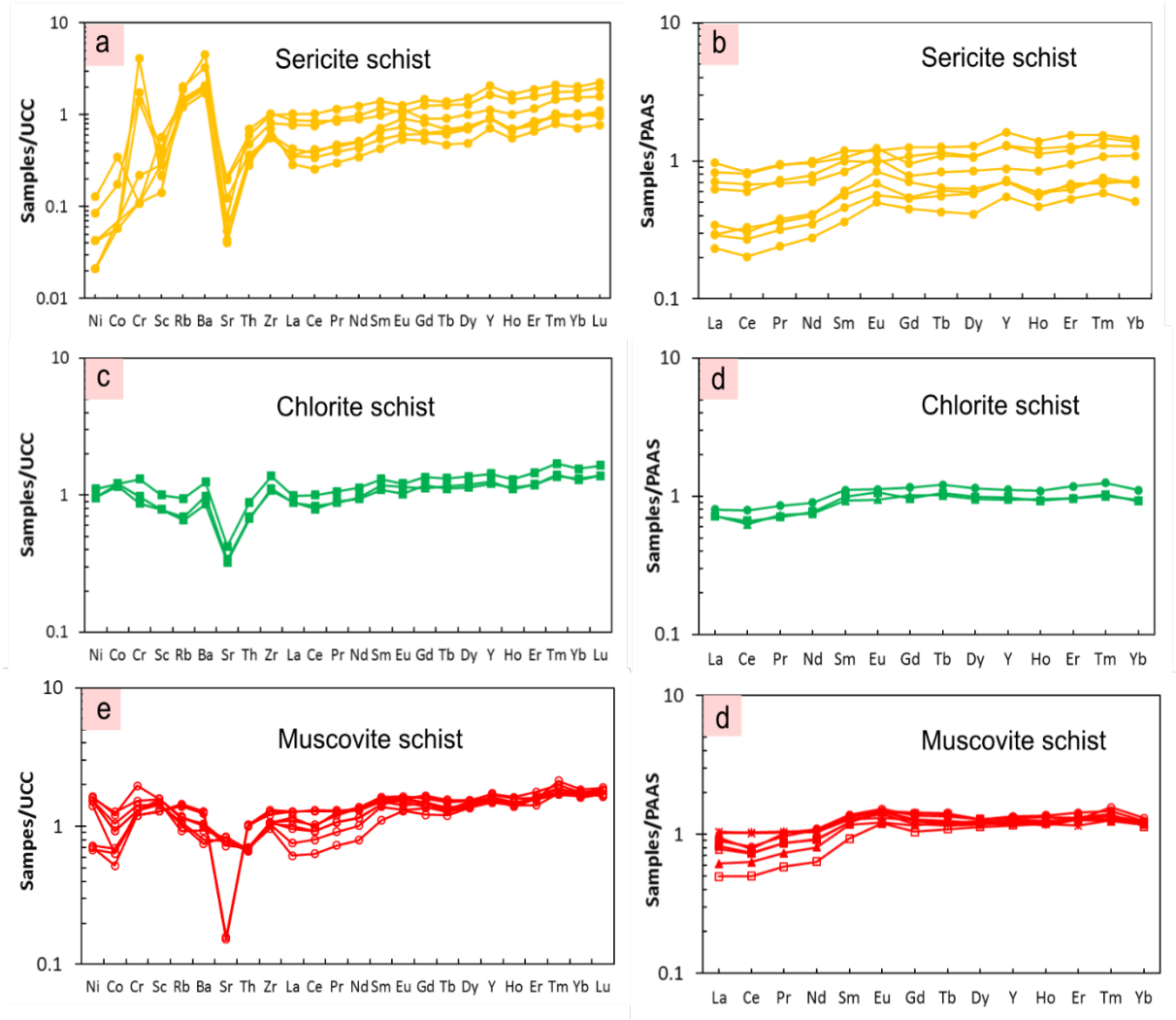

Figure 7. a, c and e: UCC-normalized multi-element patterns (normalizing values after [64]); b, d and f: PAAS-normalized REE patterns (normalizing values after [62])

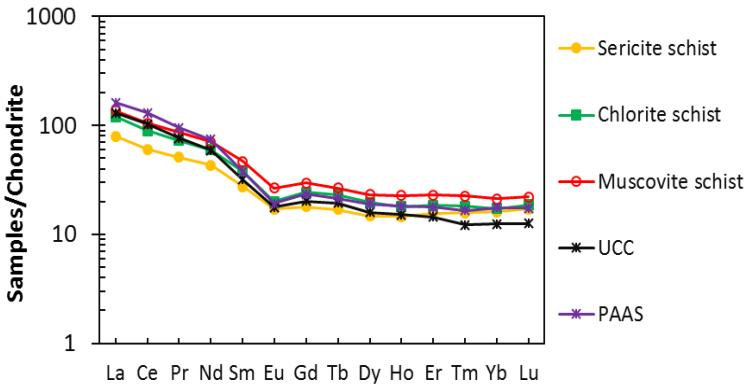

Figure 8. Comparative chondrite-normalized REE patterns of Mbondo-Ngazi Tina rocks to UCC and PAAS

6. Discussion

6.1. Element Mobility Evaluation

The Mbondo-Ngazi Tina metasediments have undergone greenschist facies metamorphism. Therefore it is fundamental to evaluate the effect of metamorphism on the mobility of major and trace elements before any geochemical interpretations. Some geochemical elements in metamorphic rocks are mobilized by effect of fluids, solid-state diffusion and melt generation [36]. At large scale, the effect of solid-state diffusion of elements is negligible and that the main effect is fluid-controlled mobility. Several lines show evidence against large-scale remobilization some elements in the analyzed samples. For examples, the studied samples show a relative linear trend on the binary diagram (Figure 5 and Figure 6), suggesting the chemical coherence and uniformity of the data and therefore argue against any large scale remobilization for these elements. Furthermore, high field

strength elements (Th, Zr, Hf, Ti, Nb, Ta) and REEs, are sometimes considered to be relatively immobile elements [37,38] and they are not significantly modified during chemical weathering and diagenesis. The REE-normalized plots display smooth REE patterns (Figure 7), which would not be expected during remobilization. In addition transition trace elements (Cr, Ni, V, Co, Sc) and high field strength elements (Zr, Nb, Hf, Ta) show consistent inter-relationships (not shown), suggest less remobilization of elements. Although it is possible that some elements such as large ion lithophile elements may have been remobilized, it is unlikely that large-scale remobilization of the REEs and the HFSE have occurred. From the above results, we infer that the studied metasediments have retained their initial geochemical signature. Thus their geochemical compositions can be used to discuss their provenance and tectonic setting.

6.2. Source-area Weathering

Many geological factors influence the chemical composition of clastic sediments. These factors includes source rock composition, the intensity of weathering, the rate of sediment supply and sorting during transportation and deposition, and finally post-depositional weathering [39,40]. The intensity of chemical weathering of sedimentary rocks can be quantified by the Chemical Index of Alteration (CIA; [41]) or the Chemical Index of Weathering (CIW; [42]) which measures the extent of conversion of feldspars to clays. In most of the case, unweathered igneous rocks are characterized by CIA values ranging from 35 to 55% for both basaltic and granitic rock respectively, and values of 60 - 80% indicate moderate weathering while values greater than 80% indicate extreme weathering at the source area [43]. The CIA values of the Mbondo-Ngazi Tina metasedimentary vary from 59.71 to 74.82 (average = 69.44) in sericite schists and from 72.30 to 80.19 (average = 74.94) in chlorite-schists and muscovite-schists. These CIA values are relative high when compared to NASC (58) and Archean greywacke (58), but close to the CIA value of PAAS (70) and cratonic sandstone (69), and but lower than that of cratonic shales (77) [44]. This would indicate that the source rocks of the Mbondo-Ngazi Tina metasedimentary rocks underwent minor to moderate chemical weathering.

In order to determine the intensity of chemical weathering for the studied rocks, the plagioclase index of alteration (PIA) and the chemical index of weathering (CIW) have been calculated. The high PIA values (> 95%) of the sericite schists indicate complete transformation of plagioclase into aluminous clay minerals like kaolinite and illite [43], suggesting high intensity of chemical weathering at source area. Furthermore, the studied metasedimentary rocks show CIW value similar to the CIA for sericite schists. High CIW values (> 80%) for chlorite schists and muscovite schists indicate intense weathering at source area [44]. Since the CIW values of the chlorite schists and muscovite schists are much higher than the CIA values, the studied samples might have experienced K-metasomatism.

Data are plotted on the $A1_2O_3$-CaO + Na_2O-K_2O (A-CN-K) ternary plot of [41,45] which is a graphic presentation of the Chemical Index of Alteration (Figure 9). In this diagram, the studied samples display two distinct weathering trends: sericite schists samples plot along the A-K boundary between biotite and muscovite composition, whereas chlorite schist and muscovite schist samples follow the granodiorite weathering trend (Figure 9). The apparent enrichment in K in sericite schists may be attributed to hydrothermal alteration (K-metasomatism). This observation confirms the fact that the chlorite schist and muscovite schist samples are extensively weathered relative sericite schists.

In sedimentary rocks, intense weathering in source areas or sediment recycling exhibit Th/U values greater than 4.0 [46]. The Th/U ratios generally increase with increasing degrees of weathering due to oxidation and the loss of uranium. The Mbondo-Ngazi Tina rocks display Th/U ratio ranging from 1.85 to 8.26. In the Th/U vs Th diagram [46], the studied rocks define two groups of samples, straddling the upper crust value (Figure 10a). The first group of samples has Th/U ratios lower than those of upper crust and fall into the depleted mantle sources field, while the second group has Th/U ratios > 4 and follows the weathering trend. These features indicate that the metasedimentary rocks of Mbondo-Ngazi Tina are had suffered varying degrees of weathering.

6.3. Sedimentary Processes and Maturation

Sedimentary processes lead to the modification of mineral abundances and consequently the concentrations of specific elements. In sedimentary rocks, SiO_2/Al_2O_3 value is generally up to 6 while in igneous rocks this ratio ranges from 3 to 5 [47]. In addition, using the empirical discrimination ratio, the variability of the $100TiO_2/Zr$ ratio is a sensitive indicator of the intensity of sorting [48]. Accordingly, the low values of SiO_2/Al_2O_3 in the muscovite schists (3.04-3.72; average=3.47) indicate the immature nature and deposition close to the source while the high SiO_2/Al_2O_3 values (up to 11.89) of other rock samples (sericite schists and chlorite schists) indicate moderate to high degree of maturity. In addition, chlorite schist and muscovite schist samples exhibit $100TiO_2/Zr$ values up to 0.33 while sericite schists display low values (< 0.33). This feature, together with the high SiO_2/Al_2O_3 ratios, indicates geochemical maturity and consequently greater degree of sedimentary recycling of sericite schist samples.

Sedimentary rocks derived predominantly from pre-existing sedimentary rocks are characterized by zircon enrichment which can be reflected by relationships between Th/Sc and Zr/Sc [46]. The Th/Sc ratio is an indicator of chemical differentiation, while the Zr/Sc ratio measures the degree of sediment recycling, and thus the Th/Sc versus Zr/Sc plot generally reflects the extent of sedimentary sorting and recycling [49]. On this diagram muscovite schist and chlorite schist samples follow the general provenance-dependent compositional variation trend while sericite schist samples suggest the presence of heavy mineral accumulation by sediment recycling and/or sorting (Figure 10b). In general, most of the samples show higher Zr/Sc ratios (>10), suggesting some degree of sediment reworking and sorting. From the above aforementioned, the enrichment of Zr and Hf in the

analyzed samples suggests zircon accumulation and therefore supports the recycled nature of the metasedimentary rocks with little contribution of igneous rocks.

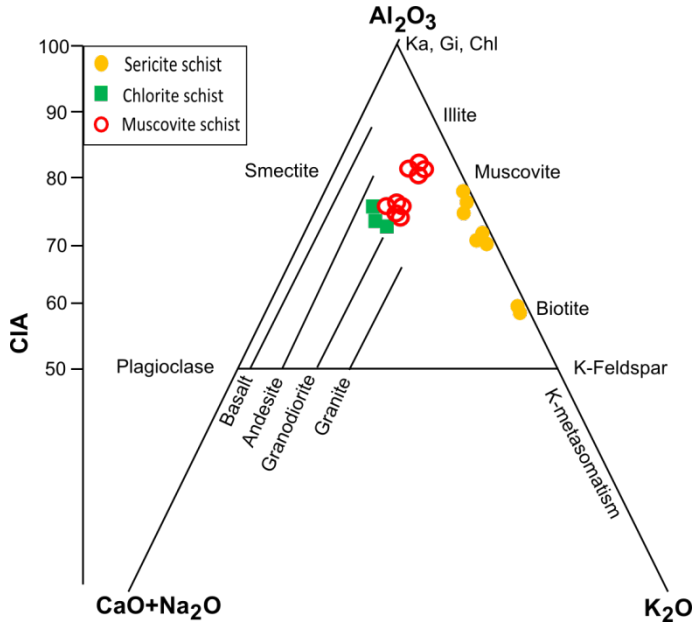

Figure 9. Molecular proportions of Al_2O_3–(Na_2O + CaO*)–K_2O ternary diagram [45] for the metasedimentary rocks of Mbondo-Ngazi Tina formations with Chemical Index of Alteration (CIA) scale

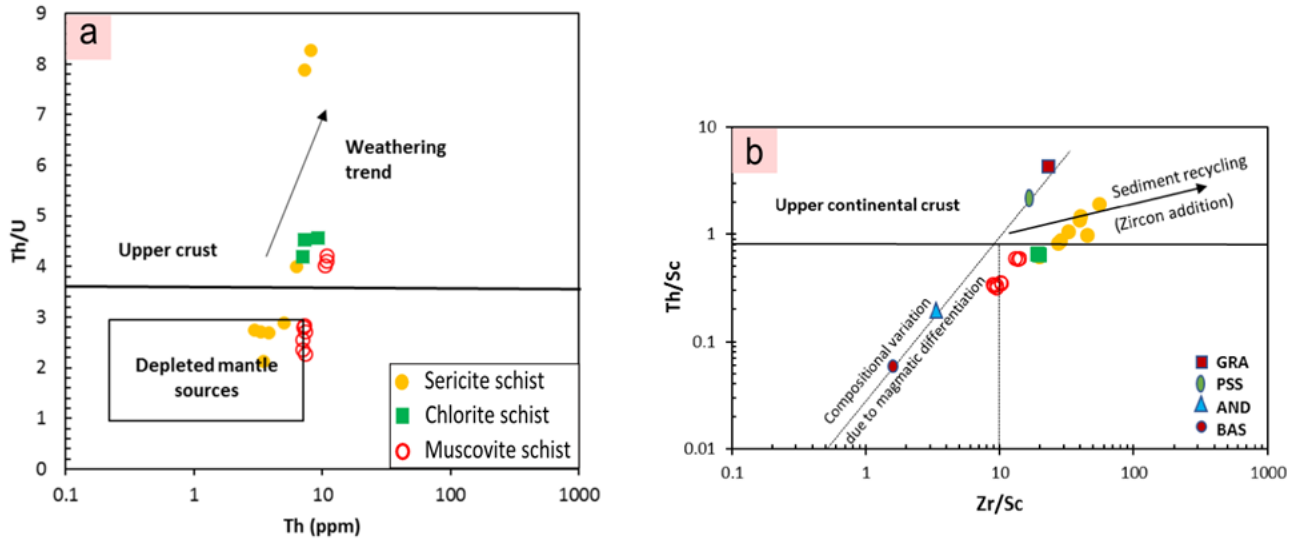

Figure 10. Plot of Th/U ratios vs. Th (a) and Th/Sc versus Zr/Sc(b) [46] Average source rock compositions are of Proterozoic age [44]. BAS, basalt; AND, andesite; GRA, granite; and PSS, Proterozoic sandstone

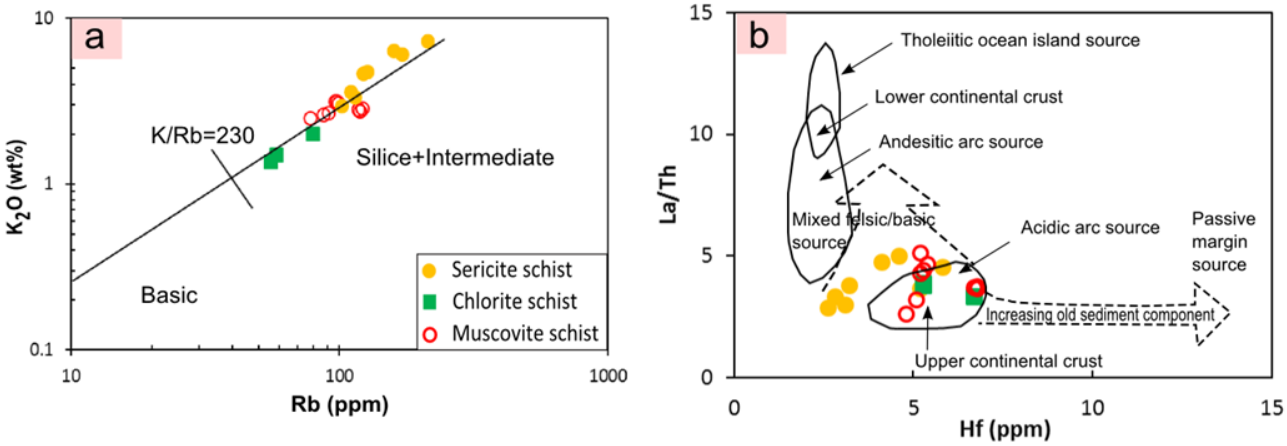

Figure 11. Source rocks discrimination diagram [56]. (a) K_2O-Rb; (b) La/Th-Hf

6.4. Provenance

Many authors [50,51,52,53,54,55] have proposed the use of Al_2O_3/TiO_2 ratio to determine the provenance of sediments due to fact that A and Ti are less affected by weathering. Al_2O_3/TiO_2 values varies from 3 to 8 in mafic rocks, from 8 to 21 in intermediate rocks and from 21 to 70 in felsic rocks. In the Mbondo-Ngazi Tina area, the Al_2O_3/TiO_2 ratio increases from chlorite schists (11.68-12.48), muscovite schists (16.53-19.21) to sericite schists (15.92-64.13) suggesting an intermediate to felsic origin of these rocks. The analysis of mafic trace element compositions shows that chlorite schists (Cr: 90-120 ppm; Ni: 45-52 ppm) and muscvite schists (Cr: 110-120; Ni: 32-77 ppm) exhibit reatively high contents when to compared to sericite schists (Cr: <10-380 ppm; Ni: <1-6 ppm). This indicates the contribution of intermediate to felsic rocks to the source of chlorite schists and muscovite schists. In addition, the Mbondo-Ngazi Tina metasediments show LREE enrichment reative to HREE and negative Eu anomaly. Their LREE/HREE ratios are low and vary from 3.84-6.51 in sericite schists, 6.70-7.18 in chlorite schists and 4-8.17 in muscovite schists, suggesting that the studied metasediments were derived from felsic to intermediate rocks. This interpretation is confirmed by the Rb-K diagram of [56], in wich all the studied rocks plot in the field of felsic/intermediate rock compositions (Figure 11a). Futhermore, when potted in the La/Th vs Hf diagram, the Mbondo-Ngazi Tina metasediments fall within the upper continental crust field and derived from old felsic sediments with minor contribution of mafic rocks (Figure 11b).

6.5. Tectonic Setting

There is a broad relationship between the geochemical characteristics of metasediments and the tectonic setting of depositional basins. Several studies [46,49,57,58,59] have attempted to distinguish the tectonic setting during deposition of sediments based on major, trace and REE data. In the K_2O/Na_2O vs. SiO_2 and SiO_2/Al_2O_3 vs. K_2O/Na_2O tectonic discrimination diagrams of [59], sericite schist samples plot into a passive continental margin field while those from chlortite schist and muscovite schist samples fall within the active continental margin and continental arc settings (Figure 12a and Figure 12b). This difference could be explained by the mobility of Na and K as it is unlikely for the rocks of the same lithological unit to have been formed in two different tectonic settings. However, continental arc and active continental margin settings are similar depositional environments as both are dominated by convergent plate motions, orogenic deformation and development of subduction complexes, and are underlain by continental crust.

McLennan et al. [60] have demonstrated that the Archean sedimentary rocks have a higher La/Th (3.6) than post-Archean sedimentary rocks (La/Th = 2.7). In the Mbondo-Ngazi Tina area, the La/Th ratios of the studied metasediments vary from 2.9 to 7.12 (average: 4.0), comparable to the Archean sedimentary rocks. This result is supported by the La vs. Th diagram (Figure 13) where all the Mbondo-Ngazi Tina metasediments are mainly plotted in the Archean sediments field. Recent investigations of the Nyong Group metasedimentary rocks in the Congo Craton have revealed that they have been deposited in active continental margin settings [61]. In this study, the provenance characteristics of the sericite schists show that they were probably deposited in a passive margin setting while chlorite schists and muscovite schists are most likely to have formed in active continental margin. Therefore, we suggest that the Mbondo-Ngazi Tina rocks derived mainly from Archean sediments and were probably deposited in an active to passive continental margin.

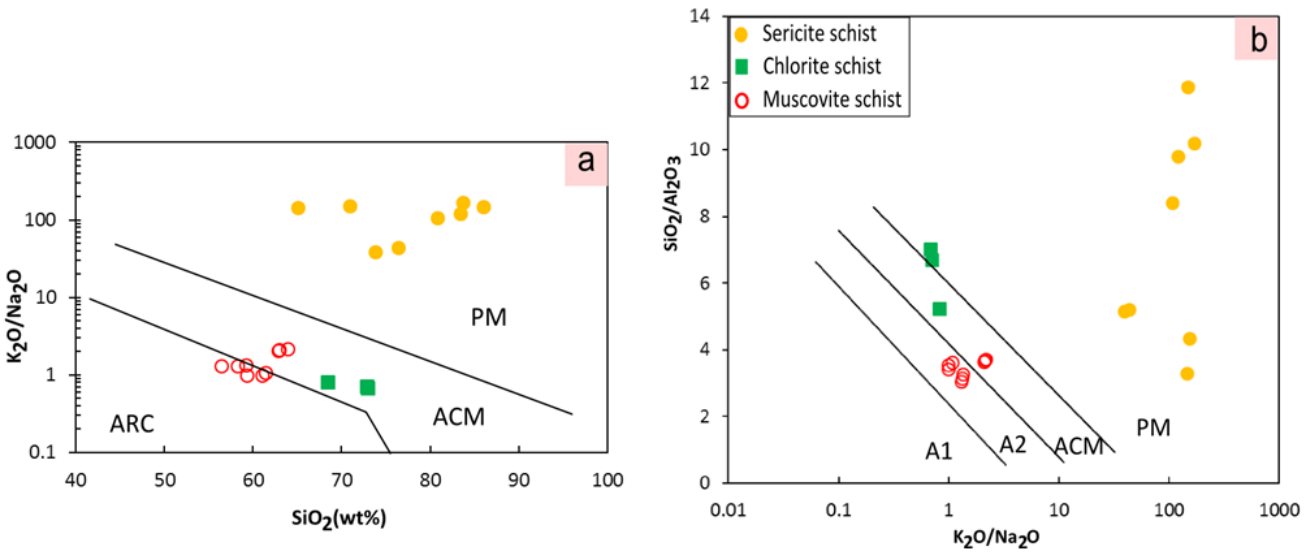

Figure 12. (a) SiO_2/Al_2O_3 vs. K_2O/Na_2O and (b) K_2O/Na_2O vs. SiO_2 [59] for tectonic discrimination diagrams of the Mbondo-Ngazi Tina metsasedimentary rocks: A1 (arc setting, basaltic and andesitic detritus), and A2 (evolved arc setting, felsic–plutonic detritus), ARC (oceanic island-arc margin), ACM (active continental margin), PM (passive margin)

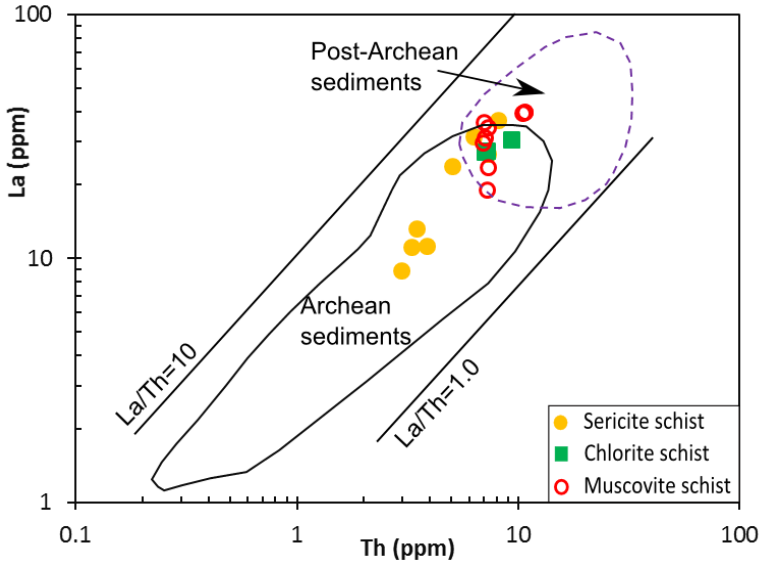

Figure 13. La vs. Th source rocks discriminating diagram for the metasedimentary rocks [62]

7. Conclusion

Whole-rock geochemical data of metasedimentary rocks from Mbondo-Ngazi Tina area indicate that they are derived from slightly immature shale to mature Fe-shale and arkose protolith, from which the original parent rock is mainly felsic to intermediate in composition. The CIA, CIW, PIA and the SiO_2/Al_2O_3 and Th/U ratios indicated that these rocks had suffered varying degrees of weathering as the source rocks underwent mild to moderate chemical weathering. They derived mainy from felsic to intermediate rocks with minor contamination of mafic rocks. The Mbondo-Ngazi Tina metasedimentary rocks show REE and trace element compositions similar to those of Archean sediments, suggesting that the continental crust of the study area during the early Proterozoic had chemical compositions similar to those of the Archean crust and were probably deposited in active to passive continental margin settings.

Acknowledgements

The data presented here form part of the first author's PhD Thesis at the Department of Earth Sciences of the University of Dschang. This research did not receive any specific grant from funding agencies in the public, commercial, or not-for-profit sectors.

References

[1] Nzenti, J.P., Njanko, T., Njiosseu, E.L.T., Tchoua, F.M., 1998. Les domaines granulitiques de la Chaîne Panafricaine Nord-Equatoriale au Cameroun. *In Géologie et environnement au Cameroun, Vicat et Bilong editors, Collection Geocam*, I, 255-264.

[2] Nzenti, J.P., Njiosseu Tanko, T. E. L., Nzina Nchare A., 2007. The metamorphic evolution of the Paleoproterozoic high grade Banyo gneisses (Adamawa, Cameroon, Central Africa). *Journal of the Cameroon Academy of Sciences*, 7, 95-109.

[3] Abdelsalam, M.G., Liégeois, J.-P., Stern, R.J., 2002. The Saharan Metacraton. *Journal of African Earth Sciences*, 34, 119-136.

[4] Toteu, S.F., Penaye, J., Djomani, Y.P., 2004. Geodynamic evolution of the Pan-African belt in central Africa with special reference to Cameroon: *Canadian Journal. Earth Sciences*, 41, 73-85.

[5] Nzenti, J.P., Barbey, P., Bertrand, J. M.L., Macaudiere, J., 1994. La chaîne panafricaine au Cameroun: cherchons suture et modèle. *In: S.G.F. édit., 15e réunion des Sciences de la Terre, Nancy, France*, 99p.

[6] Ngnotué, T., Nzenti, J.P., Barbey P., Tchoua, F.M., 2000. The Ntui Betamba high grade gneisses: a Northward extension of the pan-African Yaoundé gneisses in Cameroon. *Journal of African Earth Sciences*, 31, 369-381.

[7] Djouka-Fonkwe, M.L., Schulz, B., Nzolang, C., 2008. Geochemistry of the Bafoussam PanAfrican I- and S-type granitoids in western Cameroon. *Journal of African Earth Sciences*, 50, 148-167.

[8] Nzenti, J.P., Badibanga Kapajika, G., Wörner, Toto Ruananza Lubala, 2006. Synkinematic emplacement of granitoids in a Pan-African shear zone in Central Cameroon. *Journal of African Earth Sciences*, 45, 74-86.

[9] Nzenti, J.P., Abaga, B., Suh, C.E., Nzolang, C., 2011. Petrogenesis of peraluminous magmas from the Akum-Bamenda Massif, Pan-African Fold Belt, Cameroon. *International Geology Review*, 53(10), 1121-1149.

[10] Kwékam, M., Liégeois, J.P., Njonfang, E., Affaton, P., Hartmann, G., Tchoua, F., 2010. Nature origin and signifcance of the Pan-African high-K calc-alkaline Fomopéa plutonic complex in the Central African fold belt (Cameroon). *Journal of African Earth Sciences*, 57, 79-95.

[11] Kouankap Nono, G.D., Nzenti, J.P., Suh Cheo, E., Ganno, S., 2010. Geochemistry of ferriferous, high-K calc-alkaline magmas from the Banefo-Mvoutsaha Massif (NE Bafoussam), Central Domain of the Pan-African Fold Belt, Cameroon. *The Open Geology Journal*, 4, 15-28.

[12] Nzina Nchare, A., Nzenti, J.P., Tanko Njiosseu, E.L., Ganno, S., Ngnotué, T., 2010. Synkinematic ferro-potassic magmatism from the Mekwene-Njimafofire Foumban Massif, along the Foumban-Banyo shear zone in central domain of Cameroon PanAfrican fold belt. *Journal of Geology and Mining Research*, 2(6), 142-158.

[13] Chebeu, C., Ngo Nlend, C.D. Nzenti J-P., Ganno, S., 2011. Neoproterozoic high-K calc-alkaline granitoids from Bapa-Batié, North Equatorial Fold Belt, Central Cameroon: petrogenesis and geodynamic significance. *The Open Geology Journal*, 5, 1-20.

[14] Tchakounté, J., Eglinger, A., Toteu, S. F., Zeh, A., Nkoumbou, C. Mvondo, O.J., Penaye, J., de Wit M., Barbey, P., 2018. The Adamawa-Yadé domain, a piece of Archaean crust in the Neoproterozoic Central African Orogenic belt (Bafia area, Cameroon). *Precambrian Research*, 299, 210-229.

[15] Ngamy Kanwa, A., Tchakounte, N.J., Nkoumbou, C., Owona, S., Tchouankoue, J.P, Mvondo Ondoa, J., 2019. Petrology and

geochemistry of the Yoro-Yangben Pan-African granitoid intrusion in the Archaean Adamawa-Yade crust (SW-Bafia, Cameroon). *Journal of African Earth Sciences*, 150, 401-414.

[16] Tanko Njiosseu, E.L., Nzenti, J.P., Njanko, T., Kapajika, B., Nédelec, A., 2005. New U-Pb zircon ages from Tonga (Cameroon): coexisting Eburnean-Transamazonian (2.1 Ga) and Pan-African (0.6 Ga) imprints. *Comptes Rendus Géosciences*, 337, 551-562.

[17] Ganwa, A., Frisch, W., Siebel, W., Shang, C.K., Mvondo, O.J., Satir, M., Tchakounte, N.J, 2008a. Zircon ^{207}Pb-^{206}Pb evaporation ages of Pan-African metasedimentary rocks in the Kombé-II area (Bafia Group, Cameroon): constraints on protolith age and provenance. *Journal of African Earth Sciences*, 51, 77-88.

[18] Ganwa, A.A., Klötzli, US., Diguim Kepnamou, A., Hauzenberger, C., 2018. Multiple Ediacaran tectono-metamorphic events in the Adamawa-Yadé Domain of the Central Africa Fold Belt: Insight from the zircon U-Pb LAM-ICP-MS geochronology of the metadiorite of Meiganga (Central Cameroon). *Geological Journal*, 53(6), 2955-2968.

[19] Tchakounté, J., Eglinger, A., Toteu, S. F., Zeh, A., Nkoumbou, C. Mvondo, O.J., Penaye, J., de Wit M., Barbey, P., 2017. The Adamawa-Yadé domain, a piece of Archaean crust in the Neoproterozoic Central African Orogenic belt (Bafia area, Cameroon). *Precambrian Research*, 299, 210-229.

[20] McLennan, S.M., Hemming, S., Taylor, S.R., Eriksson, K. A., 1995. Early Proterozoic crustal evolution: geochemical and Nd-Pb isotopic evidence from metasedimentary rocks, southwest ern North America. *Geochimica et Cosmochimica Acta*, 59, 1153-1177.

[21] Tchaptchet Tchato D., Nzenti J.P, Njiosseu E. L., Ngnotué, T, Ganno S., 2009. Neoproterozoic metamorphic events in the kekem area (Central domain of the Cameroon North Equatorial Fold Belt): P-T data. *Journal of the Cameroon Academy of Sciences*, 8(2/3), 91-105.

[22] Dickinson, W. R., Suczek, C. A., 1979. Plate tectonics and sandstone compositions. *Bull. Am. Assoc. Pet. Geol*., 63, 2164-2182.

[23] Dickinson, W. R., Beard, L. S., Brakenridge, G. R., Erjavec, J. L., Ferguson, R. C., Inman, K. F., Knepp, R. A., Lindberg, F. A., Ryberg, P. T., 1983. Provenance of North America Phanerozoic sandstone in relation to tectonic setting. *Bull. Geol. Soc. Am*., 94, 222-235.

[24] Toteu, S.F., Van Schmus, W.R., Penaye, J., 2006b. The Precambrian of Central Africa: Summary and perspectives: *Journal of African Earth Sciences*, 44, 7-10.

[25] Van Schmus, W.R., Oliveira, E.P., Da Silva Filho, A.F., Toteu, S.F., Penaye, J., Guimaraes, I.P., 2008. Proterozoic links between the Borborema Province, NE Brazil, and the Central African Fold Belt.*Geol. Soc. London, Spec. Publ.*, 294(1), 69-99.

[26] Nzenti, J.P., Barbey, P., Macaudiere, J., Soba, D., 1988. Origin and evolution of late Precambrian high - grade Yaounde gneisses (Cameroon). *Precambrian Research*, 38, 91-109.

[27] Toteu, S.F., Van Schmus, W.R., Penaye, J., Nyobé, J.B., 1994. U-Pb and Sm-N evidence for Eburnian and Pan-African high-grade metamorphism in cratonic rocks of southern Cameroon: *Precambrian Research*, 67, 321-347.

[28] Toteu, S.F., Penaye, J., Deloule, E., Van Schmus, W.R., Tchameni, R., 2006a. Diachronous evolution of volcanosedimentary basins north of the Congo craton: Insights from U-Pb ion microprobe dating of zircons from the Poli, Lom and Yaoundé Groups (Cameroon): *Journal of African Earth Sciences*, 44, 428-442.

[29] Ngnotue, T., Ganno, S., Nzenti, J.P., Schulz, B., Tchaptchet Tchato, D., Suh Cheo, E., 2012. Geochemistry and geochronology of peraluminous High-K granitic leucosomes of Yaounde series (Cameroon): evidence for a unique Pan-African magmatism and melting event in North-Equatorial Fold Belt. *International Journal of Geosciences*, 3(3), 525-548.

[30] Metang, V., 2015. *Cartographie géologique du secteur de Matomb-Makak (Centre-sud Cameroun): Implications sur l'évolution géodynamique du groupe panafricain de Yaoundé* (Unpublished Thesis). Université de Yaoundé I, 263p.

[31] Toteu, S.F., Van Schmus, W.R., Penaye, J., Michard, A., 2001. New U-Pb and Sm-Nd data from north-central Cameroon and its bearing on the prePan-African history of central Africa: *Precambrian Research*, 108, 45-73.

[32] Hamdja Ngoniri, A., Soh Tamehe, L., Ganno, S., Ngnotue, T., Zuxing Chen, Huan Li, Ayonta Kenne, P., Nzenti, JP. Geochronology and petrogenesis of the Pan-African granitoids from Mbondo-Ngazi Tina in the Adamawa-Yadé Domain, Central Cameroon. *International Journal of Earth Sciences, submitted*.

[33] Tchameni, R., Pouclet, A., Penaye, J., Ganwa, A.A., Toteu, S.F., 2006. Petrography and geochemistry of the Ngaoundéré Pan-African granitoids in Central North Cameroon: Implications for their sources and geological setting. *Journal of African Earth Sciences* 44, 511-529.

[34] Winchester, J. A., Park, K. G., Holland, J. G., 1980. The geochemistry of Levisian semipelitic schists from the Gairloch district western Ross. *Scottish Journal of Geology*, 16, 165-179.

[35] Herron, M.M., 1988. Geochemical classification of terrigenous sands and shales from core or log data. *Journal of Sedimentary Petrology*, 58, 820-829.

[36] Rollinson, H.R. (1993). Using Geochemical Data: Evolution, Presentation, Interpretation. *Longman, Essex, England*, 1-352.

[37] Pearce, J.A., 1996. A user's guide to basalt discrimination diagrams. In: Wyman, D.A. (Ed.), Trace Element Geochemistry of Volcanic Rocks: Application for Massive Sulphide Exploration. *Mineralogical Association of Canada, Short Course*, 12, 79-113.

[38] Taylor, S.R., McLennan, S.M., 1985. The Continental Crust: Its Composition and Evolution. *Blackwell Scientific Publishers, Oxford*.

[39] Cullers, R.L., Bock, B., Guidotti, C., 1997. Elemental distribution and neodymium isotopic compositions of Silurian metasediments, western Maine, USA: redistribution of the rare earth elements. *Geochimica et Cosmochimica Acta*, 61, 1847-1861.

[40] Roddaz, M., Viers, J., Brusset, S., Baby, P., Boucayrand, C., Hérail, G., 2006. Controls on weathering and provenance in the Amazonian foreland basin: insights from major and trace element geochemistry of Neogene Amazonian sediments. *Chemical Geology*, 226, 31-65.

[41] Nesbitt, H.W., Young, G.M., 1982. Early Proterozoic climates and plate motions inferred from major element chemistry of lutites. *Nature*, 299, 715-717.

[42] Harnois, L., 1988. The CIW index: a new chemical index of weathering. *Sedimentary Geology*, 55, 319-322.

[43] Fedo, C.M., Nesbitt, H.M., Young, G.M., 1995. Unraveling the effects of potassium metasomatism in sedimentary rocks and paleosols, with implications for paleoweathering conditions and provenance. *Geology*, 23, 921-924.

[44] Condie, K.C., 1993. Chemical composition and evolution of the upper continental crust: contrasting results from surface samples and shales. *Chemical Geology*, 104, 1-37.

[45] Nesbitt, H.W., Young, G.M., 1989. Formation and diagenesis of weathering profiles. *Journal of Geology*, 97, 129-147.

[46] McLennan, S. M., Hemming, S., McDaniel, D. K., Hanson, G.N., 1993. Geochemical approaches to sedimentation, provenance and tectonics. In: Johnsson, M.J., Basu, A. (Eds.), Processes Controlling the Composition of Clastic Sediments. *Geological Society of America Special Paper*, 284, 21-40.

[47] Roser, B.P., Cooper, R.A., Nathan, S., Tulloch, A. J., 1996. Reconnaissance sandstone geochemistry, provenance, and tectonic setting of the lower Paleozoic terranes of the West Coast and Nelson, New Zealand. *Journal of Geology and Geophysics*, 39, 1-16.

[48] Garcia, D., Fonteilles, M., Moutte, J., 1994. Sedimentary fractionations between Al, Ti, and Zr and the genesis of strongly peraluminous granites. *Journal of Geology*, 102, 411-422.

[49] McLennan, S.M., Taylor, S.R., McCulloch, M.T., Maynard, J.B., 1990. Geochemical and Nd-Sr isotopic composition of deep-sea turbidites: crustal evolution and plate tectonic associations. *Geochimica et Cosmochimica Acta*, 54, 2015-2050.

[50] Broecker, W.S., Peng, T-H., 1982. Tracers in the Sea. *Lamont-Doherty Geological Observatory Columbia University, Palisades, New York*, 10964.

[51] Girty, G.H., Ridge, D.I., Knaack, C., Johnson, D., Al-Riyami, R.K., 1996. Provenance and Depositional Setting of Paleozoic Chert and Argillite, Sierra Nevada, California. *Journal of Sedimentary Research*, 66, 107-118.

[52] Hayashi, K., Hiroyuki, F., Heinrich, H.D., Ohmoto, H., 1997. Geochemistry of 1.9 Ga sedimentary rocks from northeastern Labrador, Canada. *Geochimica et Cosmochimica, Acta*, 61, 4115-4137.

[53] Qiao, Y., Hao, Q., Peng, S., Wang, Y., Li, J., Liu, Z., 2001.

Geochemical Characteristics of the Eolian Deposits in Southern China, and their Implications for Provenance and Weathering Intensity. *Palaeogeography, Palaeoclimatology, Palaeoecology*, 308, 513-523.

[54] Sheldon, N.D., Tabor, N.J., 2009. Quantitative Paleoenvironmental and Paleoclimatic Reconstruction Using Paleosols. *Earth-Science Reviews*, 95, 1-52.

[55] Nagarajan, R., Armstrong -Altrin, J.S., Kessler, F.L., Hidalgo-Moral, E.L., Dodge-Wan, D., Taib, N.I., 2015. Provenance and tectonic setting of Miocene siliciclastic sediments, Sibuti Formation, Northwestern Borneo. *Arabian Journal of Geosciences*, 8, 8549-8565.

[56] Floyd P.A., Winchester, J.A., Park, R.G., 1989. Geochemistry and tectonic setting of Lewisian Clastic Metasediments from the Early Proterozoic Loch Maree Group of Gairloch, NW Scotland. *Precambrian Research*, 45, 203-214.

[57] Bhatia, M.R., 1983. Plate tectonics and geochemical composition of sandstone. *Journal of Geology*, 91, 611-627.

[58] Bhatia, M.R., Crook, K.A., 1986. Trace element characteristics of greywackes and tectonic setting discrimination of sedimentary basins. *Contribution to Mineralogy and Petrology*, 92, 181-193.

[59] Roser, B.P., Korsch, R.J., 1986. Determination of tectonic setting of sandstone-mudstone suites using SiO_2 content and K_2O/Na_2O ratio. *Journal of Geology*, 94, 635-650.

[60] McLennan, S.M., Taylor, S.R., 1980. Th and U in sedimentary rocks: crustal evolution and sedimentary recycling. *Nature*, 285, 62l-624.

[61] Soh Tamehe, L., Nzepang, T.M., Wei, C.T., Ganno, S., Ngnotue, T., Kouankap, N.G.D., Simon, S.J., Zhang, J.J., Nzenti, J.P., 2018. Geology and geochemical constrains on the origin and depositional setting of Kpwa-Atog Boga banded iron formations (BIFs), northwestern Congo craton, southern Cameroon. *Ore Geology Reviews*, 95, 620-638.

[62] McLennan, S.M., 1989. Rare earth elements in sedimentary rocks: influence of provenance and sedimentary processes. In: Lipin, B.R., McKay, G.A. (Eds.), Geochemistry and Mineralogy of Rare Earth Elements. Rev. Miner. Geochem., pp. 169–200.

[63] Gromet, L.P., Dymek, R.E., Haskin, L.A., Korotev, R.L., 1984. The North American shale composite: its composition, major and trace element characteristics. *Geochimica et Cosmochimica Acta*, *48*, 2469-2482.

[64] Rudnick, R.L., Gao, S., 2003. The composition of the continental crust. In: Rudnick, R.L. (Ed.), The Crust. Elsevier-Pergamon, Oxford, pp. 1-64.